Modelization of nitrogen diffusion induced by the formation of a surface carbonitride layer

Nathalie Millard-Pinard, Nathalie Moncoffre, Henri Jaffrezic, Gilbert Marest

▶ **To cite this version:**

Nathalie Millard-Pinard, Nathalie Moncoffre, Henri Jaffrezic, Gilbert Marest. Modelization of nitrogen diffusion induced by the formation of a surface carbonitride layer. Japanese Journal of Applied Physics, 1993, 74 (10), pp.6032-6038. 10.1063/1.355218 . in2p3-00013034

HAL Id: in2p3-00013034

https://in2p3.hal.science/in2p3-00013034v1

Submitted on 28 Oct 2024

HAL is a multi-disciplinary open access archive for the deposit and dissemination of scientific research documents, whether they are published or not. The documents may come from teaching and research institutions in France or abroad, or from public or private research centers.

L'archive ouverte pluridisciplinaire **HAL**, est destinée au dépôt et à la diffusion de documents scientifiques de niveau recherche, publiés ou non, émanant des établissements d'enseignement et de recherche français ou étrangers, des laboratoires publics ou privés.

Distributed under a Creative Commons Attribution - NonCommercial - NoDerivatives 4.0 International License

Modelization of nitrogen diffusion induced by the formation of a surface carbonitride layer

N. Millard-Pinard, N. Moncoffre, H. Jaffrezic, and G. Marest
Institut de Physique Nucléaire de Lyon, IN2P3-CNRS et Université Claude Bernard 43, Bd du 11 Novembre 1918, 69622 Villeurbanne Cedex, France

Nitrogen implantations were performed into iron at a fluence of 10^{17} ^{15}N cm^{-2}, an energy of 50 keV, a temperature of 150 °C, two vacuum pressures (2×10^{-3} and 6×10^{-5} Pa), and five current densities (6, 18, 24, 40, 60 $\mu A\ cm^{-2}$). Experimental profiles display a preferential nitrogen migration towards the surface. In order to interpret the variation of the depth distribution shapes versus the pressure and the current density, a calculation model is elaborated. This model takes into account the presence of the contamination carbon at the sample surface. A comparison between experimental and simulated profiles is presented. An interpretation of the carbon role is proposed. The different hypothesis on the nitrogen migration mechanisms are reviewed.

I. INTRODUCTION

Improvement of tribological properties (specially wear resistance) of iron or steels after nitrogen implantation is now well established. Some authors attribute this improvement to dispersed nitrides inside the matrix, other authors to the formation of carbonitrides in the outermost layers.[1–6] An interpretation of the mechanism by which carbon is incorporated from the residual gas into the sample surface has been suggested by Singer.[1] In a very recent paper we have discussed the carbon diffusion during nitrogen implantation in iron under different conditions of fluences and beam current densities. This study did not take into account the carbonitride formation.[7]

Nitrogen migration towards the surface when the target temperature is in the range 80–200 °C has been also often studied.[8–11] However, the mechanism by which nitrogen atoms migrate preferentially towards the surface compared to the bulk is still discussed. In particular Jagielski *et al.*[12] have demonstrated that the most likely mechanism is a radiation-induced segration in which nitrogen-vacancy complexes migrate towards vacancy sinks (the sample surface for example).

In our implantation conditions at the Nuclear Physic Institute of Lyon, a strong carbon contamination at the sample surface has always been observed and carbonitrides have been detected by conversion electron Mössbauer spectroscopy (CEMS).[6,7] These observations suggest that carbon could play an important role in the increased nitrogen precipitation at the surface. Hence, in this paper, we propose a model which takes into account this carbon contamination and whose purpose is to simulate the nitrogen diffusion towards the surface during implantations at 150 °C.

II. EXPERIMENTAL CONDITIONS

In order to favor nitrogen migration, nitrogen ions were implanted in iron at a controlled temperature of 150 °C, with 50 keV energy and at a fluence of 10^{17} ^{15}N cm^{-2}. Previous studies[8] show that in these conditions a nitrogen surface peak is clearly distinguished. Moreover, at this temperature, the carbon contamination and the carbonitride formation are enhanced whereas no stable nitrogen-rich Fe_2N phase is formed. The beam current density was varied in the 6–60 $\mu A\ cm^{-2}$ range and the implantations were performed under two different vacuums: the first one ($\sim2\times10^{-3}$ Pa) leads to a high carbon contamination level whereas the second one ($\sim6\times10^{-5}$ Pa) is obtained by introducing a cold finger around the sample holder. The carbon concentrations were measured using nuclear backscattering spectrometry (NBS) with 5.7 MeV α particles. These C concentrations were already published (for example: for 24 $\mu A\ cm^{-2}$, $C=7.4\times10^{16}$ at cm^{-2} in the bad vacuum and $C=7.2\times10^{15}$ at cm^{-2} in the good vacuum). It was verified that the oxygen pollution was negligible.[7] Nitrogen depth profiles were determined by using the resonant nuclear reaction $^{15}N(p,\alpha\gamma)^{12}C$ at 429 keV. In order to corroborate the measured nitrogen profiles with the carbonitride formation CEMS experiments were performed.

III. EXPERIMENTAL RESULTS

The nitrogen profiles are presented here after as a function of the vacuum quality during implantation.

A. High carbon contamination level

The nitrogen profiles obtained after implantations of 10^{17} ions cm^{-2} at 150 °C and in a 2×10^{-3} Pa pressure are shown in Fig. 1 for 6, 18, 24, 40, and 60 $\mu A\ cm^{-2}$ current densities. These results have been previously presented.[7] The beam current density influences of course the implantation duration. These durations were varied within the 222–22 min range.

Figure 1 clearly demonstrates the crucial effect of current density on nitrogen distributions which are divided into two parts: a broad peak located at around 70 nm corresponding to the TRIM predictions and a surface peak. The surface peak is all the more important that the current density is low, i.e., the implantation duration is

Accepted Manuscript

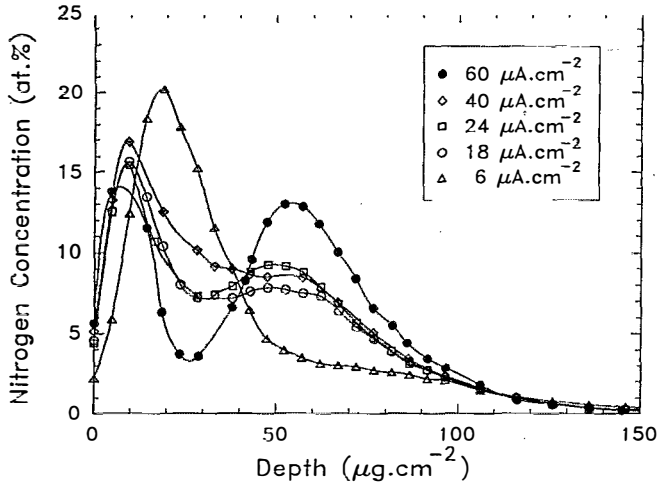

FIG. 1. Nitrogen depth distributions obtained using the $^{15}N(p,\alpha\gamma)^{12}C$ resonant nuclear reaction for the various current densities ($\Phi=10^{17}$ N cm^{-2}, $E=50$ keV, $T=150$ °C, $P=(2\pm1)\times10^{-3}$ Pa).

long. For example, for 6 μA cm^{-2}, 60% of the implanted nitrogen is contained in the superficial peak (as also confirmed by Mössbauer spectroscopy which indicates the relative abundance of carbonitride phases) whereas for 60 μA cm^{-2}, only 23% of nitrogen atoms have reached the surface. The same tendency was observed for 5×10^{6} and 2×10^{17} ions cm^{-2} fluences.

B. Low carbon contamination level

At the pressure of 6×10^{-5} Pa, the nitrogen depth profiles were also measured for the 6, 18, 24, and 40 μA cm^{-2} current density conditions. The results are presented in Fig. 2. For the three lower current density values the distributions are very similar and only display a single peak at the very near surface. Such profile shapes were never observed in the previous vacuum conditions. At 40 μA cm^{-2},

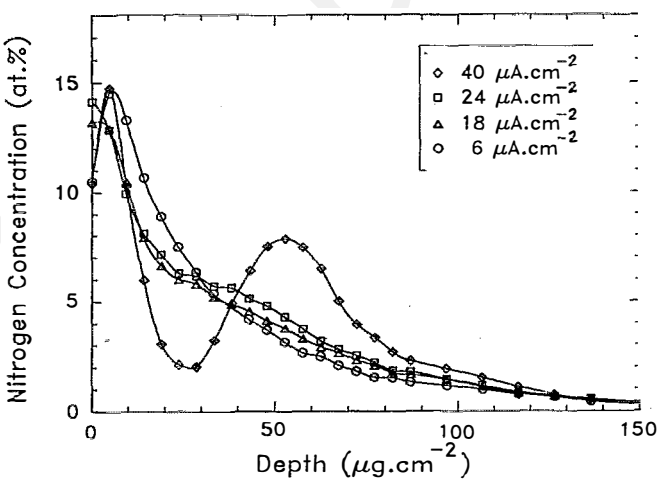

FIG. 2. Nitrogen depth distributions obtained using the $^{15}N(p,\alpha\gamma)^{12}C$ resonant nuclear reaction for the various current densities ($\Phi=10^{17}$ N cm^{-2}, $E=50$ keV, $T=150$ °C, $P=(6\pm2)\times10^{-5}$ Pa).

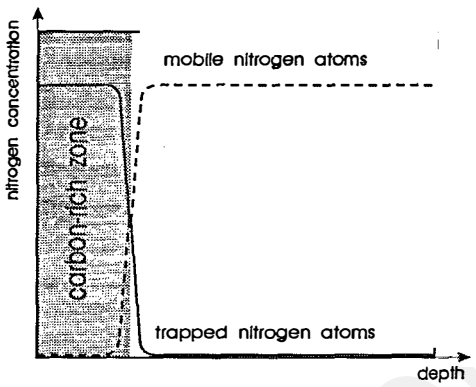

FIG. 3. Schematic representation of the different carbon and nitrogen species localization inside the implanted zone.

the surface peak is obvious together with the broader distribution located at 65 nm from the surface.

From these results the effect of the vacuum quality and consequently of the surface carbon contamination on the nitrogen profile evolution is clearly demonstrated.

On the basis of this experimental study, we have elaborated a calculation model whose purpose is to simulate the nitrogen profiles presented above.

IV. DIFFUSION MODEL

Let us assume that in iron, nitrogen and carbon exist under two forms:

(1) free nitrogen or carbon atoms which we call mobile nitrogen or carbon and which are noted N_d or C_d,

(2) bound nitrogen and carbon atoms which are embedded in carbonitride phases. These species are noted N_c and C_c, respectively.

At the relatively low dose of 10^{17} N cm^{-2}, the nitride formation is neglected compared to the carbonitride one. It is worth noting that CEMS analysis has identified the carbonitride compounds as mainly $\epsilon-Fe_{2+x}(C,N)$ phases.[13–15]

At any depth and at any time, the nitrogen or carbon concentrations are

$$C_N = C_{N_d} + C_{N_c}, \tag{1}$$

$$C_C = C_{C_d} + C_{C_c}. \tag{2}$$

During implantation the mobile nitrogen that diffuses towards the surface bounds with superficial carbon atoms and consequently the mobile nitrogen concentration at the surface is equal to 0. Hence a nitrogen concentration gradient constantly exists inside the implanted region. This process is schematized in Fig. 3.

Let us consider an elementary cylinder having a Δx length, a unit section, and consequently a Δx volume.[16]

The variation of the total nitrogen amount inside the cylinder during the Δt time is

$$\Delta C_N \Delta x = (J_{N_x} - J_{N(x+\Delta x)})\Delta t, \tag{3}$$

Not Manuscript

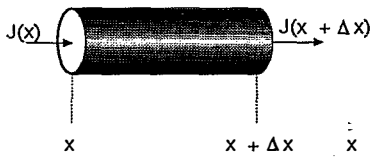

FIG. 4. Schematic representation of the incoming and outgoing nitrogen fluxes through an elementary cylinder.

J_{N_x} and $J_{N(x+\Delta x)}$ being the incoming and outgoing nitrogen fluxes as illustrated in Fig. 4.

Now,

$$J_{N_x}=J_{N_{dx}}+F(x)\Delta x, \tag{4}$$

where $J_{N_{dx}}$ is the flux of mobile nitrogen and $F(x)$ is the contribution of nitrogen brought by implantation. The outgoing nitrogen is obviously mobile, hence

$$J_{N(x+\Delta x)}=J_{N_{d(x+\Delta x)}} \tag{5}$$

and then

$$\Delta C_N \Delta x=(J_{N_{dx}}-J_{N_{d(x+\Delta x)}})\Delta t+F(x)\Delta x\Delta t. \tag{6}$$

$J_{N_{dx}}-J_{N_{d(x+\Delta x)}}$ being the variation of the mobile nitrogen flux inside the cylinder, one can write

$$J_{N_{dx}}-J_{N_{d(x+\Delta x)}}=D_N\frac{\partial^2 C_{N_d}}{\partial x^2}\Delta x. \tag{7}$$

since $J_{N_d}=-D_N\,\partial C_{N_d}/\partial x$, where D_N is the nitrogen diffusion coefficient ($cm^2\,s^{-1}$).

Consequently

$$\frac{\partial C_N}{dt}=D_N\frac{\partial^2 C_{N_d}}{\partial x^2}+F(x). \tag{8}$$

Taking into account the surface sputtering, $F(x)$ is expressed as

$$F(x)=\frac{i}{\sqrt{2\pi}\Delta R_{p_N}}\exp-\frac{(x-R_{p_N}-a\Phi)^2}{2(\Delta R_{p_N})^2}, \tag{9}$$

where i is the number of impinging ions per cm^2 and per second ($i=6.25\times10^{12}j$ where j is the current density in $\mu A\,cm^{-2}$), R_{p_N} is the projected range of nitrogen ions ($R_{p_N}=57$ nm at 50 keV in iron), Φ is the implanted fluence at a certain time t and $a\Phi$ ($g\,cm^{-2}$) is the sputtered depth, a being the sputtered mass per incident ion. After a total implanted fluence Φ_0, the surface shift is $a\Phi_0$ and $a\Phi$ (nm) $=7.39\times10^{-4}Yjt$, Y being the sputtering yield.

If we assume that the kinetics of carbonitride formation is of the first order in comparison with C_{N_d} and C_{C_d}, it can be written

$$\frac{\partial C_{N_C}}{\partial t}=k_N C_{N_d} C_{C_d}, \tag{10}$$

$$\frac{\partial C_{C_C}}{\partial t}=k_C C_{N_d} C_{C_d}, \tag{11}$$

with k_N and k_C ($cm^3\,s^{-1}$) defined as the velocity constants of carbonitride formation relative to nitrogen and carbon, respectively.

Thus from Eq. (1),

$$\frac{\partial C_N}{\partial t}=\frac{\partial C_{N_d}}{\partial t}+\frac{\partial C_{N_C}}{\partial t}, \tag{12}$$

$$\frac{\partial C_C}{\partial t}=\frac{\partial C_{C_d}}{\partial t}+\frac{\partial C_{C_C}}{\partial t}, \tag{13}$$

then from Eqs. (12), (8), and (10),

$$\frac{\partial C_{N_d}}{\partial t}=D_N\frac{\partial^2 C_{N_d}}{\partial x^2}-k_N C_{N_d} C_{C_d}+F(x). \tag{14}$$

Moreover, assuming that carbon atoms are distributed according to a thin Gaussian shape at the near surface and that the rate of incoming atoms is U_0 (at $cm^{-2}\,s^{-1}$)

$$G(x)=\frac{U_0}{\sqrt{2\pi}\Delta R_{p_C}}\exp-\frac{(x-a\Phi)^2}{2(\Delta R_{p_C})^2}, \tag{15}$$

where ΔR_{p_C} is the straggling of the carbon distribution.

Thus

$$\frac{\partial C_{C_d}}{\partial t}=D_C\frac{\partial^2 C_{C_d}}{\partial x^2}-k_C C_{N_d} C_{C_d}+G(x), \tag{16}$$

D_C being the carbon diffusion coefficient.

The system constituted by the four following equations was resolved by a NAG routine:

$$\frac{\partial C_{N_C}}{\partial t}=k_N C_{N_d} C_{C_d},$$

$$\frac{\partial C_{C_C}}{\partial t}=k_C C_{N_d} C_{C_d},$$

$$\frac{\partial C_{N_d}}{\partial t}=D_N\frac{\partial^2 C_{N_d}}{\partial x^2}-k_N C_{N_d} C_{C_d}+F(x),$$

$$\frac{\partial C_{C_d}}{\partial t}=D_C\frac{\partial^2 C_{C_d}}{\partial x^2}-k_C C_{N_d} C_{C_d}+G(x).$$

V. COMPARISON BETWEEN THEORETICAL AND EXPERIMENTAL PROFILES

This model being established, it has been used to determine theoretical profiles with parameters corresponding to the experimental conditions:

$\Phi=10^{17}$ N cm^{-2}, $E=50$ keV, $T=150$ °C in the two different vacuum pressures (2×10^{-3} and 6×10^{-5} Pa) and the four different current densities (6, 18, 24, 40, or 60 $\mu A\,cm^{-2}$).

A. High carbon contamination conditions

The experimental (empty symbols) and theoretical (full symbols) nitrogen profiles together with the carbon distributions deduced from the fits are shown in Figs. 5 and 6 for the different current density values j.

Accepted Manuscript

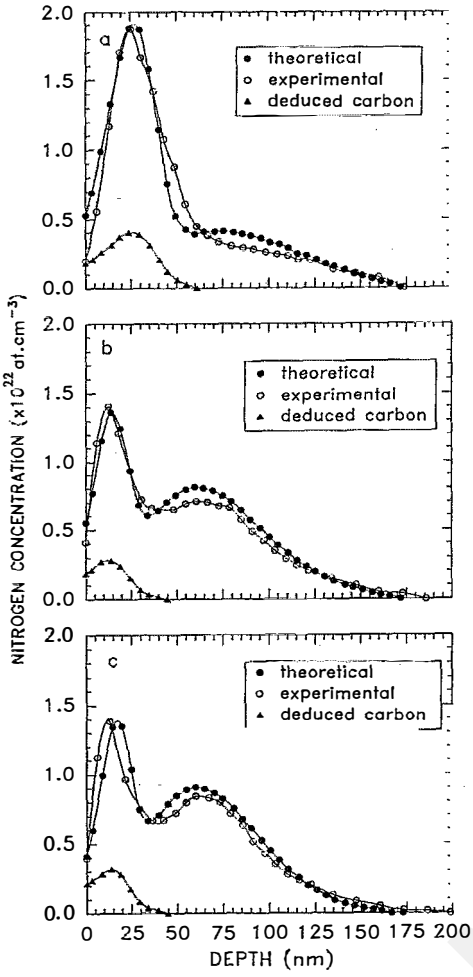

FIG. 5. Simulation of experimental profiles obtained in the high carbon contamination conditions, $\Phi = 10^{17}$ N cm^{-2}, $T = 150$ °C: (a) 6 μA cm^{-2}, $U_0 = 1.3\times10^{12}$ at cm^{-2} s^{-1}, N/C=7; (b) 18 μA cm^{-2}, $U_0 = 2.2\times10^{12}$ at cm^{-2} s^{-1}, N/C=16; (c) 24 μA cm^{-2}, $U_0 = 3.4\times10^{12}$ at cm^{-2} s^{-1}, N/C=14. The other parameters are fixed: $D_N = D_C = 3\times10^{-15}$ cm^2 s^{-1}, $k_N = 2.6\times10^{-23}$ cm^3 s^{-1}, $k_C = 0.5\times10^{-23}$ cm^3 s^{-1}, $Y = 0.7$.

For the three lower beam current densities (6, 18, 24 μA cm^{-2}) good fits are obtained with the parameter values reported in the figure caption. The following parameters: D_N, D_C, k_N, k_C, and Y were maintained constant, whereas only U_0 was varied from one fit to another. It is worth noting that k_C is smaller than k_N indicating that the precipitates are nitrogen-rich carbonitrides. Indeed, Mössbauer spectroscopy measurements have detected magnetic components corresponding to $Fe_{2.55}$ $(C_{0.08}N_{0.92})$ precipitates.[17] The increase of U_0 as a function of j can be understood since the carbon diffusion is all the more important when the j value is high, i.e., the implantation duration is short.

For 6 μA cm^{-2}, the theoretical N/C ratio is equal to 7, i.e., that 1.3×10^{16} C cm^{-2} can diffuse. As experimentally the total carbon concentration has been evaluated to be 1.8×10^{17} at cm^{-2} (Table I) we assume that for a low beam current density a large amount of carbon contamination is not radiolyzed and therefore does not diffuse.

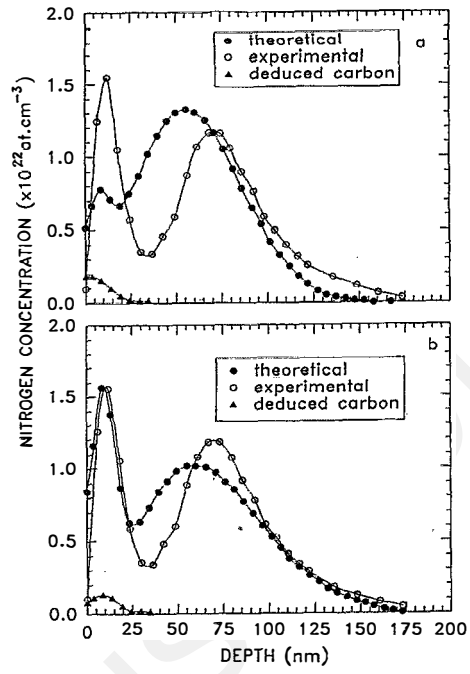

FIG. 6. Simulation of the experimental profile obtained in the high carbon contamination conditions for 60 μA cm^{-2}, $\Phi = 10^{17}$ N cm^{-2}, $T = 150$ °C. (a) same fixed parameters than for 6, 18, and 24 μA cm^{-2} with $U_0 = 3.4\times10^{12}$ at cm^{-2} s^{-1}, N/C=47; (b) higher diffusion coefficients and velocity constants of carbonitride formation $U_0 = 2.0\times10^{12}$ at cm^{-2} s^{-1}, N/C=58, $D_N = D_C = 9\times10^{-15}$ cm^2 s^{-1}, $k_N = 50\times10^{-23}$ cm^3 s^{-1}, $k_C = 4\times10^{-23}$ cm^3 s^{-1}.

Identical observations are available for the 18 and 24 μA cm^{-2} current densities as shown in Table I.

The fit performed with the same fixed parameters for the profile obtained at 60 μA cm^{-2} is not satisfactory [Fig. 6(a)]. Obviously nitrogen is more mobile than simulated. This enhanced mobility could be due to a temperature raise of the near surface which could accelerate nitrogen and carbon diffusion and favor carbonitride formation. One can note that for this high j value the global sample temperature is probably increased but this increase is not observed due to the unperfect thermal contact between the sample and its holder. For this reason, the D_N, D_C, k_N, k_C parameter values were increased [Fig. 6(b)] to significantly

TABLE I. Measured or calculated parameters (rate of incoming carbon atoms U_0, remaining nitrogen dose N, theoretical N/C ratio, mobile carbon amount, and total carbon amount) corresponding to nitrogen implantations in the high carbon contamination conditions as a function of the current density.

Current density (μA cm^{-2})	6	18	24	60
U_0 (at cm^{-2} s^{-1})	1.3×10^{12}	2.2×10^{12}	3.4×10^{12}	2.0×10^{12}
Remaining dose N (at cm^{-2})	9.1×10^{16}	8.8×10^{16}	9.1×10^{16}	1.0×10^{17}
Theoretical ratio N/C	7	16	14	58
Mobile carbon amount (at cm^{-2})	1.3×10^{16}	5.5×10^{15}	6.5×10^{15}	1.7×10^{15}
Total carbon amount (at cm^{-2})	1.8×10^{17}	1.1×10^{17}	7.5×10^{16}	1.8×10^{15}

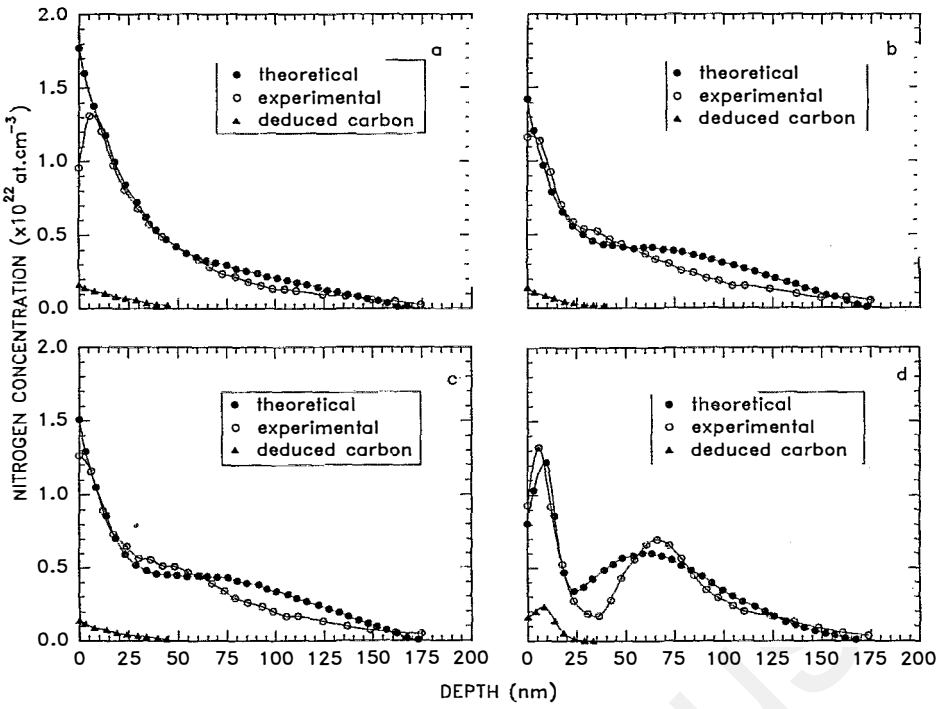

FIG. 7. Simulation of the experimental profiles obtained in the low carbon contamination level, $\Phi=10^{17}$ N cm^{-2}, $T=150$ °C: (a) 6 μA cm^{-2}, $T=150$ °C, $U_0=1.5\times10^{11}$ at cm^{-2} s^{-1}, N/C=20; (b) 18 μA cm^{-2}, $U_0=0.5\times10^{12}$ at cm^{-2} s^{-1}, N/C=41; (c) 24 μA cm^{-2}, $U_0=0.8\times10^{12}$ at cm^{-2} s^{-1}, N/C=40. The other parameters are fixed: $D_N=35\times10^{-15}$ cm^2 s^{-1}, $D_C=8.0\times10^{-15}$ cm^2 s^{-1}, $k_N=5.0\times10^{-23}$ cm^3 s^{-1}, $k_C=0.5\times10^{-23}$ cm^3 s^{-1}, $Y=0.7$.

improve the fit. From the increase of the D_N diffusion coefficient it is possible to evaluate the temperature raise using the Arrhenius law: $D_N=D_0\exp(-E/kT)$ if we assume, as it will be proposed in the discussion, that nitrogen migrates towards the surface bound with vacancy clusters which activation energy is 1.28 eV.[18] With this value the new parameter would correspond to a temperature raise of 24 degrees. In this new fit U_0 was also changed to 2×10^{12} at cm^{-2} s^{-1}. This lower value can be justified by an increase of the carbon sputtering at 60 μA cm^{-2} and thus the amount of free carbon is diminished. Indeed, the unbound carbon concentration (1.7×10^{15} at cm^{-2}) estimated from the theoretical N/C ratio equal to 58 is very weak and Mössbauer data from the literature[17] show that carbonitrides are carbon poorer than the phases produced at 6 μA cm^{-2}.

It is worth noting that at 60 μA cm^{-2}, the nitrogen distribution around R_p is narrower than theoretically predicted. The fact that nitride formation is not considered in our model could explain this disagreement. For long implantation durations, the nitrogen concentration at the top of the Gaussian distribution is lower since the diffusion process has time to occur. On the contrary for high beam current densities, the diffusion time is diminished and consequently a larger amount of nitrogen atoms are immobilized around R_p. However, on each side of this high nitrogen concentration zone, implanted atoms remain mobile and by diffusion contribute to the growing of surface carbonitrides and nitrides located in the central peak. Such a narrowing of nitrogen profiles has already been pointed out by Barnavon *et al.* for nitrogen-implanted samples after post-annealings under vacuum.[19]

B. Low carbon contamination conditions

A second set of experiments was performed in the cleaner vacuum. The experimental and theoretical nitrogen profiles together with carbon distributions deduced from the fits are displayed in Fig. 7 for the 6, 18, 24, and 40 μA cm^{-2} beam current densities. At this pressure, the remaining nitrogen dose is about 6.1×10^{16} at cm^{-2} instead of 9.2×10^{16} at cm^{-2} in the high carbon contamination level (Table I). Since this nitrogen loss is not taken into account in our model, it could explain the relative quality of the fits.

For the three lower j values the experimental profiles, almost similar, are again fitted by varying U_0 only. Nitrogen and carbon diffusion coefficients (D_N and D_C) have larger values than when the contamination level is high. In this last case, the low value of D_C is justified by the abundant amount of carbon (and oxygen) atoms which slow down the carbon diffusion. With regard to nitrogen atoms as their outdiffusion is not considered in our model, the D_N increase seems to be due to an enhanced diffusion. The larger calculated D_N value is certainly artificial.

Like for implantations performed in high carbon contamination conditions, mobile carbon concentrations obtained from theoretical N/C ratios are always less than the total carbon concentrations deduced from NBS measurements (Table I). However, as these values are weak it

Accepted Manuscript

would be dangerous to speculate about them.

For 40 μA cm^{-2} the experimental nitrogen depth distribution is narrower than the theoretical one as it was observed for the high contamination conditions at 60 μA cm^{-2}. Again the narrowing of the peak can be explained by a nitride formation which reduces the nitrogen atom diffusion process. Since the existence of these nitrides is not taken into account in our model, this could explain the change in the D_N, D_C, k_N, and k_C adjusted values.

VI. DISCUSSION

The nitrogen diffusion coefficient values introduced in the different simulations are always in the range 3×10^{-15} to 3.5×10^{-16} cm^2 s^{-1}. Now, from the literature[20] the interstitial diffusion coefficient of nitrogen in α iron at 150 °C is equal to 1.1×10^{-12} cm^2 s^{-1}. From these data we can assume that nitrogen atoms do not only migrate according to an interstitial diffusion mechanism.

To explain this nitrogen diffusion towards the surface, several hypothesis have already been proposed. We will remind them briefly.

(i) Piette[18] interprets the surface peak as a result of a fast nitride precipitation due to the presence of a large vacancy concentration near the surface. Nitrogen atoms could be trapped by vacancy clusters and these formed complexes could initiate the iron nitride precipitation. This model confers an essential role to vacancies in the nitride precipitation but these vacancies are not necessary in the nitrogen migration process since the author assumes that nitrogen atoms diffuse interstitialy in iron. Moreover, Piette does not explain why vacancies are concentrated in the near surface region and why these defects do not annihilate at the surface itself.

(ii) A theoretical model based on a coupling between the impurity and defect fluxes has been proposed by Rangaswamy *et al.*[21] Nevertheless taking into account the nitride formation, the authors by this model did not well reproduce the experimental depth profiles obtained by Moncoffre *et al.*[8] and Singer *et al.*[3]

(iii) With Jagielski[12] we propose that the nitrogen redistribution is due to the radiation-induced segregation mechanism in which nitrogen atoms migrate bound with vacancies (so called Miller's pairs[22]) towards the sample surface. To justify the diffusion of Miller's pairs, the authors assume the existence of a large vacancy concentration gradient in the implanted zone implying a superficial vacancy concentration equal to zero,[12] the vacancy annihilation at the surface being due to the rearrangement of the outermost atomic layer.

Our model is based on the existence of a nitrogen concentration gradient inside the sample with mobile atoms and bound atoms in the carbonitride phases. However, it does not discuss the mechanism itself of nitrogen migration. In fact, we comfort the Miller's pairs formation hypothesis but it is likely that nitrogen does not migrate under this form only. Indeed the nitrogen diffusion coefficient at 150 °C is found rather small ($D_N = 16\times10^{-15}$ cm^2 s^{-1}) deduced from our fits. Hence nitrogen diffusion could be due to two coexisting mechanisms: interstitial diffusion of N atoms, migration of Miller's pairs.

The migration of Miller's pairs is not a unique mechanism in which the redistribution of nitrogen atoms may be due to the radiation-induced segregation. Another possibility which can be involved is the formation of mixed dumbbells (i.e., complexes of nitrogen and self interstitial atoms).[23] Nitrogen atoms would diffuse complexed with interstitial iron atoms. However, our results do not allow us to discuss in detail this question.

Moreover, the intense compressive stresses induced by the implantation process could be also a driving force acting on nitrogen atoms.

In conclusion, in this paper, we have shown that nitrogen depth distributions after implantations at 150 °C in two different vacuums and with various current densities are correctly described taking into account: the existence of carbon contamination at the sample surface, the formation of carbonitrides, the presence of a nitrogen concentration gradient inside the implanted region.

The various hypothesis proposed to explain the nitrogen diffusion mechanism have been reviewed. Concerning the enhanced precipitation of nitrogen atoms at the surface, we have proposed as an explanation the carbonitride formation. However, the trapping of nitrogen by vacancy clusters has also to be considered.

ACKNOWLEDGMENTS

The authors would like to thank sincerely Professor J. Tousset who has initiated the calculation model for his competence. We wish him a nice retirement. We also thank J. Jagielski for interesting and helpful discussions and A. Plantier who performed the implantations.

[1] I. L. Singer, J. Vac. Sci. Technol. A **1**, 419 (1983).
[2] I. L. Singer, Appl. Surf. Sci. **18**, 28 (1984).
[3] I. L. Singer, Vacuum **34**, 853 (1984).
[4] C. A. Dos Santos, M. Behar, and I. J. R. Baumvol, J. Phys. D **17**, 551 (1984).
[5] M. Iwaki, Mater. Sci. Eng. **90**, 263 (1987).
[6] G. Marest, Defect and Diffusion Forum **53-58**, 273 (1988), and references herein.
[7] N. Millard-Pinard, H. Jaffrezic, G. Marest, N. Moncoffre, and J. Tousset (unpublished).
[8] N. Moncoffre, G. Hollinger, H. Jaffrezic, G. Marest, and J. Tousset, Nucl. Instrum. Methods B **7-8**, 177 (1985).
[9] B. Rauschenbach, Nucl. Instrum. Methods B **15**, 756 (1986).
[10] G. Terwagne, M. Piette, F. Bodard, and W. Möller, Mater. Sci. Eng. A **115**, 25 (1989).
[11] J. Jagielski, G. Gawlik, A. Podgorski, A. Turos, A. Dygo, and N. Madi, Phys. Status Solidi A **112**, 343 (1989).
[12] J. Jagielski, N. Moncoffre, G. Marest, L. Thomé, A. J. Barcz, G. Gawlik, and W. Rosinski (unpublished).
[13] R. Frattini, G. Principi, S. Lo Russo, B. Tivernon, and C. Tosello, J. Mater. Sci. **17**, 1683 (1982).
[14] G. M. Chen, N. K. Jaggi, J. B. Butt, E. B. Yek, and L. N. Schwartz, J. Phys. Chem. **87**, 5326 (1983).
[15] S. M. M. Ramos, L. Amaral, M. Behar, G. Marest, A. Vasquez, and F. C. Zawislak, Mater. Sci. Eng. A **115**, 31 (1989).
[16] Y. Adda and J. Philibert, (Presses Universitaires de France, Paris 1966).
[17] D. Firrao, G. Principi, M. Rosso, and R. Frattini, Proceedings of the International Conference on the Applications of the Mössbauer Effect, 1982, p. 218.

[18] M. Piette, Diplôme de Doctorat, Université Notre-Dame de la Paix, Namur, 1990.
[19] Th. Barnavon, H. Jaffrezic, G. Marest, N. Moncoffre, J. Tousset, and S. Fayeulle, Mater. Sci. Eng. **69**, 531 (1985).
[20] J. R. G. da Silva and R. B. McLellan, Mater. Sci. Eng. **26**, 83 (1976).
[21] M. Rangaswamy, D. Farkas, and H. L. Sobel, Nucl. Instrum. Methods Phys. Res. B **19/20**, 196 (1987).
[22] A. D. Le Claire, J. Nucl. Mater. **69/70**, 70 (1979).
[23] P. N. Dederichs, C. Lehmann, H. R. Schober, A. Scholz, and R. Zeller, J. Nucl. Mater. **69/70**, 176 (1978).

Accepted Manuscript